International Journal of Biology and Life Sciences
ISSN: 2957-9511 | Vol. 10, No. 1, 2025

Analysis of Microbial Community Structure in Different Rotting Regions of Wax Apple

Yu Huang *, Hongbo Zhang, Shan Liu

School of Environmental Ecology and Biological Engineering, Wuhan University of Engineering, Wuhan, Hubei, 430000, China
* **Corresponding author**: Yu Huang (Email: Huangyu1419@163.com)

Abstract: With the rapid development of the tropical fruit industry, wax apple (*Syzygium samarangense*) has emerged as an economically important crop in southern China due to its distinctive flavor and high nutritional value. However, systematic investigations into microbial community dynamics during its spoilage remain scarce. In this study, high-throughput sequencing was employed to analyze microbial community structures in wax apples at three distinct decay stages. Results demonstrated that bacterial alpha-diversity significantly increased in decayed tissues while fungal diversity declined, with both showing reduced diversity in later stages—a microbial succession pattern analogous to those observed in grapes and blueberries. Notably, fungi likely dominate spoilage initiation by adapting to the host microenvironment through activation of glyoxylate cycle, toxin biosynthesis, and antioxidant defense pathways, mirroring the pathogenesis of *Botrytis cinerea*. Conversely, bacteria accelerated decay progression by upregulating virulence-associated pathways such as membrane transport and xenobiotic degradation. Bacterial-derived pectinase/cellulase decomposed cell walls to release monosaccharides as fungal carbon sources, while fungal metabolites reciprocally sustained bacterial growth, suggesting a potential synergistic cross-kingdom interaction network. Healthy tissues maintained microbial homeostasis through basal metabolism and antimicrobial compound biosynthesis, exhibiting 1.7-fold higher energy metabolism pathway activity compared to decayed tissues. This study pioneers the characterization of fungal-bacterial dynamics in wax apple spoilage, predicts disease-resistant mechanisms in healthy fruits, and provides theoretical insights for developing targeted antimicrobial preservation strategies.

Keywords: Wax Apple; Postharvest Decay; Microbial Community; High-throughput Sequencing.

1. Introduction

As a representative tropical berry fruit, wax apple (*Syzygium samarangense*) is rich in diverse bioactive components that provide optimal conditions for microbial proliferation [1], leading to postharvest challenges including enzymatic browning, tissue softening, and pathological deterioration [2]. Conventional culture-dependent approaches, while traditionally employed in fruit spoilage microorganism research, exhibit inherent limitations such as inadequate sensitivity and incomplete taxonomic classification, thereby constraining comprehensive elucidation of microbial community dynamics during decay processes.

Recent advances in metagenomic sequencing technologies, particularly 16S rRNA/ITS high-throughput sequencing [3.4], have revolutionized postharvest microbiome research due to their superior resolution and high-throughput capabilities[5-7]. Wang et al.[8] demonstrated through high-resolution sequencing that Wickerhamomyces anomalus colonizes kiwifruit endophytes and modulates bacterial community composition to suppress pathogen proliferation, thereby maintaining fruit health. Similarly, Liu et al.[9] employed sequencing analysis to reveal that high-voltage electrostatic fields significantly alter fungal community structure and enhance mycological diversity on sweet cherries. These findings underscore the transformative potential of next-generation sequencing in overcoming detection limitations of conventional methods, offering novel perspectives for deciphering microbial consortia architecture and interspecies interactions during fruit spoilage.

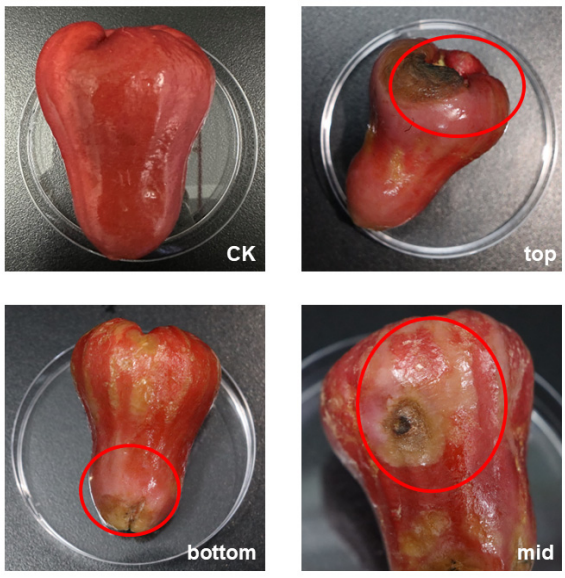

Figure 1. Diagram of Corruption of *Syzygium samarangense* Sampling

Building upon these methodological advancements, this investigation employs an integrated approach combining full-length 16S rRNA/ITS sequencing with advanced bioinformatics strategies (encompassing α/β-diversity metrics, LEfSe multivariate discriminant analysis, and PICRUSt2 functional prediction) to systematically characterize the compositional dynamics, successional patterns, and metabolic functional shifts within bacterial communities during wax apple deterioration. The findings provide critical theoretical foundations for developing targeted antimicrobial

interventions and optimizing postharvest preservation protocols, while establishing a methodological framework for microbiome studies in tropical fruits.

2. Materials and Methods

2.1. Experimental Materials

Postharvest deteriorated 'Black Diamond' wax apples were procured from a certified plantation in Sanya, Hainan Province of China. All specimens originated from a single harvest batch stored under controlled cold storage conditions (4 °C), exhibiting synchronous decay onset. Diseased fruits were transported to the laboratory within 24 h via refrigerated logistics (4 °C). Healthy controls were selected from the same harvest batch based on strict criteria: tree-ripened fruits with intact epidermis, uniform morphology, and absence of phytopathological symptoms.

2.2. Microbial DNA Extraction and Quality Assessment

Healthy fruits displayed no water-soaking lesions or discoloration, with characteristic glossy epicarp and firm texture. Three distinct decay zones were sampled (Figure 1): (A) Top (pedicel-adjacent necrosis), (B) Mid (equatorial decay), and (C) Bottom (calyx-end rot). Under aseptic conditions, 500 mg tissue from demarcated regions (Figure 1 red zones) was excised using sterilized scalpels and transferred to lysing matrix tubes. Sequential addition of 978 μ L Sodium Phosphate Buffer (pH 8.0) and 122 μ L MT Buffer preceded mechanical homogenization in a FastPrep® system (MP Biomedicals, Abe Medical Device Trading Co., Shanghai, Ltd.) with dual-phase processing: 40 s homogenization at 6.0 m/s, repeated twice. Genomic DNA was isolated using the DNeasy PowerSoil Pro Kit (Qingke Xinye Biotechnology Co., Beijing, Ltd.) per manufacturer's protocol, with final eluates stored at -20 ℃ for downstream analyses.

DNA integrity was verified via NanoDrop 2000 spectrophotometry (Thermo Fisher Scientific), with $A_{260/280}$ ratios maintained between 1.8-2.0 to ensure protein-free nucleic acid preparations. Quantification thresholds (>20 ng/μ L) were enforced to meet sequencing library preparation requirements.

2.3. Illumina MiSeq Amplicon Sequencing

Qualified DNA samples were subjected to paired-end 250 bp sequencing on the Illumina MiSeq platform (Illumina Inc., USA) through a commercial service (Guangdong Magigene Biotechnology Co., Ltd., Shenzhen, China). Bacterial 16S rRNA gene (V3-V4 hypervariable regions) and fungal ITS (ITS1-ITS2 regions) were amplified using fusion primers with platform-adapted adapters. Raw sequences were processed through QIIME2 v2022.2 (https://qiime2.org/) with the following workflow: demultiplexing, quality filtering (Q20 threshold), and denoising via DADA2[10] with optimized parameters (trim length: F230/R200; maximum expected errors: 2; chimeric sequence removal).

To mitigate host-derived interference, all features taxonomically annotated as "Mitochondria" or "Chloroplast" were systematically excluded from the amplicon sequence variant (ASV) table prior to downstream analyses. Taxonomic classification was performed using pre-trained Naïve Bayes classifiers integrated in QIIME2: the SILVA 138 database for bacterial profiling and the UNITE database for fungal identification. Microbial community visualization was implemented in R v4.3.0 using the ggplot2 package v3.5.0, with phylogenetic trees constructed via FastTree2 for beta-diversity metrics.

3. Result

3.1. Microbial Community Profiling

This study conducted amplicon sequencing of 16S rRNA and ITS regions on wax apple samples from three distinct decay stages. The rarefaction curves (Good's coverage) for both 16S rRNA and ITS sequencing exceeded 99%, confirming the reliability of sequencing depth in representing microbial community characteristics (Figure 2). For 16S rRNA amplicon sequencing, 2,136,307 total sequences were obtained from 12 samples, with 1,867,013 high-quality sequences retained after denoising and filtering (average length: 362 bp). The effective sequences per sample ranged from 92,105 to 243,657 (mean: 155,584), clustered into 223 amplicon sequence variants (ASVs). As shown in Figure 3, 14 ASVs were shared across all 12 samples. Blank controls and treatment groups exhibited 15, 52, 69, and 24 unique bacterial ASVs, representing 6.73%, 23.3%, 30.9%, and 10.8% of total ASVs, respectively.

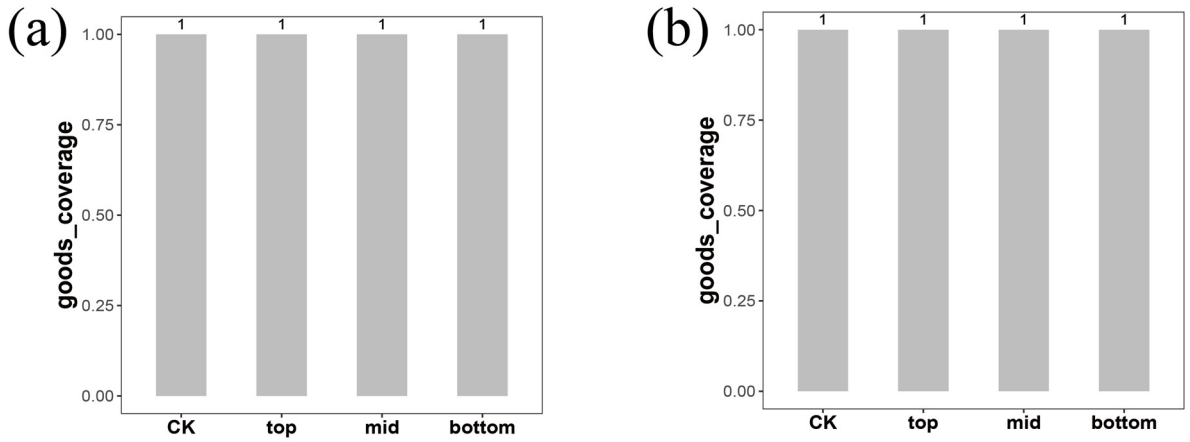

Figure 2. Sample sequencing dilution curve depth plot
(a) Bacterial 16S rRNA sequencing data (b) Fungal ITS sequencing data

For ITS amplicon sequencing, 1,887,614 total sequences were acquired, yielding 1,704,456 high-quality sequences

(average length: 314 bp) after processing. Sample-specific sequences ranged from 53,347 to 220,402 (mean: 142,038), classified into 187 fungal ASVs. Figure 2b demonstrates 24 shared fungal ASVs among all samples. Blank controls and treatment groups contained 32, 15, 37, and 24 unique fungal ASVs, constituting 17.1%, 8.02%, 19.8%, and 12.8% of total ASVs, respectively.

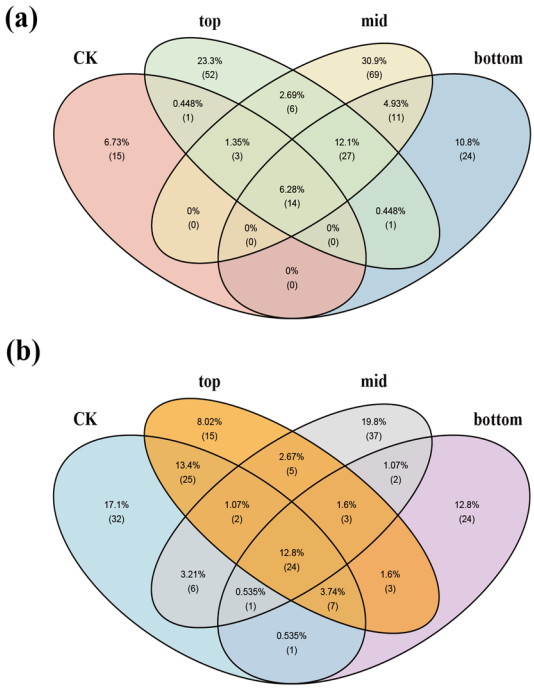

Figure 3. Venn diagram of shared ASVs in the microbial communities of *Syzygium samarangense* samples across different health conditions and three distinct stages of decay: (a) Shared ASVs in the bacterial community. (b) Shared ASVs in the fungal community

3.2. Microbial Community Structure and Composition

Bacterial ASVs obtained from all samples were taxonomically annotated at the genus level. Figure 4 displays the top 15 most abundant bacterial taxa: *Asaia*, *Pantoea*, *Gluconobacter*, *Desulfobacterota* (phylum), *Dyella*, *Kluyvera*, *Rhodococcus*, *Acetobacter*, *Pelomonas*, *Tatumella*, *Anaerolineaceae* (family), *Aquabacterium*, *Mycobacterium*, and *MBNT15* (phylum). Comparative analysis revealed that decayed tissues were predominantly colonized by *Asaia* (24.3-36.8%) and *Pantoea* (18.5-29.7%), whereas control (CK) tissues showed higher proportions of *Asaia* (42.1%) and *Desulfobacterota* (16.9%). Notably, current food science literature lacks direct evidence implicating *Asaia*, *Pantoea*, or *Desulfobacterota* as primary food spoilage agents or plant pathogens. The ubiquitous dominance of *Asaia* across all groups (21.4-42.1%) aligns with its known ecological niches in sugar-rich environments and insect guts (e.g., mosquitoes and fruit flies) [11], suggesting potential involvement in fruit decomposition without exhibiting classical pathogenic traits. Collectively, the absence of statistically dominant fruit-pathogenic bacteria implies bacterial infection may not constitute the principal etiology of these three decay phenotypes.

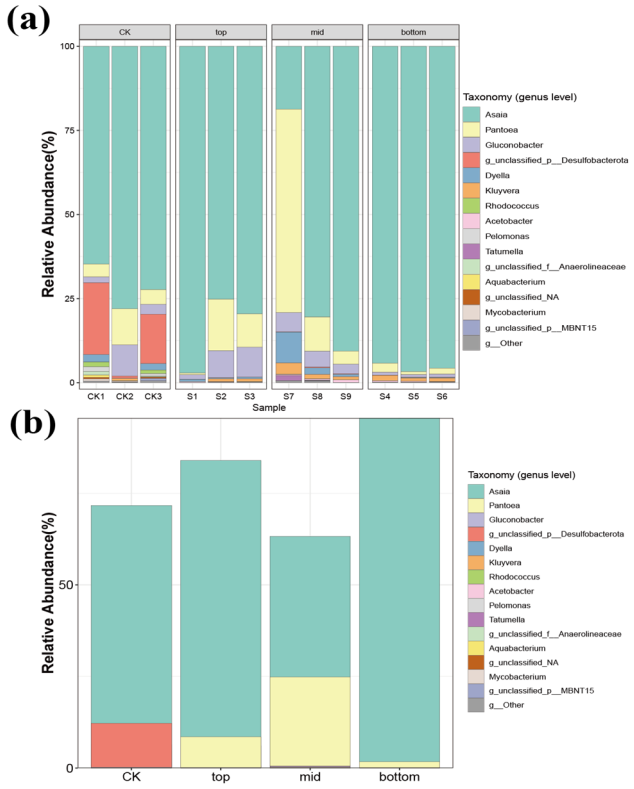

Figure 4. Relative abundance distribution maps of species of Bacteria at the Genus level for healthy and three different decay conditions of *Syzygium samarangense* samples

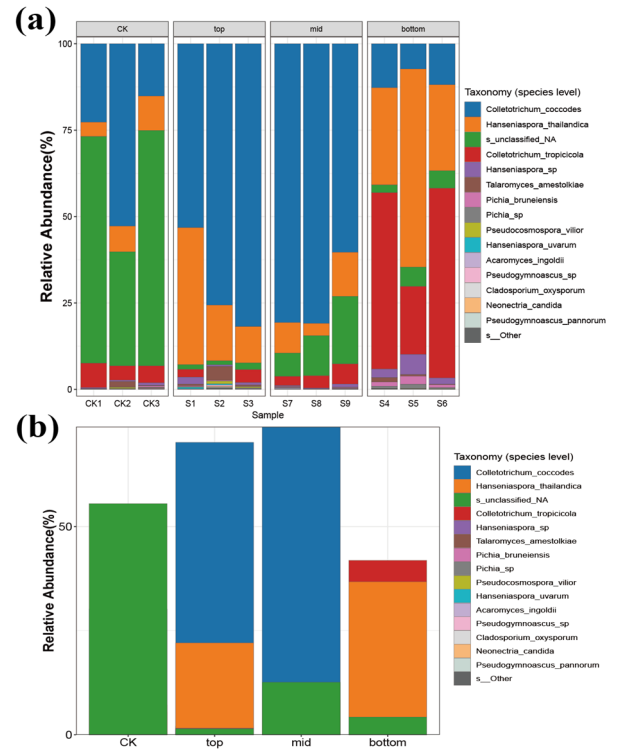

Figure 5. Relative abundance distribution maps of species of Fungi at the Species level for healthy and three different decay conditions of *Syzygium samarangense* samples

For fungal ASVs, species-level annotation identified the top 15 taxa (Figure 4): *Colletotrichum coccodes*, *Hanseniaspora thailandica*, *Colletotrichum tropicicola*, *Hanseniaspora* sp., *Talaromyces amestolkiae*, *Pichia bruneiensis*, *Pichia* sp., *Pseudocosmospora vilior*, *Hanseniaspora uvarum*, *Acaromyces ingoldii*,

Pseudogymnoascus sp., *Cladosporium oxysporum*, *Neonectria candida*, and *Pseudogymnoascus pannorum*. Significant structural divergence emerged between decayed and healthy microbiomes. Top decay tissues exhibited marked dominance of *C. coccodes* (70.22%) and *H. thailandica* (22.07%), mid decay tissues showed *C. coccodes* predominance (73.9%), while bottom decay tissues were characterized by *C. tropicicola* (41.9%) and *H. thailandica* (36.7%). Current evidence does not directly associate *Hanseniaspora* species with food spoilage pathogenesis [12], with domestic studies highlighting their antagonistic activity against *Botrytis cinerea* [13]. This suggests that despite phenotypic variation across decay regions, fungal infection likely constitutes the primary driver of wax apple spoilage.

3.3. Alpha Diversity of Microbial Communities in Decayed Wax Apples

Analysis of bacterial alpha diversity indices (Figure 6) revealed that decayed groups exhibited significantly higher Observed and Chao1 indices compared to controls (CK), indicating increased bacterial species richness during spoilage. Notably, CK and top decay groups showed significant differences in these indices. Diversity metrics (Simpson and Shannon indices) demonstrated the lowest bacterial diversity in the bottom decay group, with highly significant differences observed between CK and bottom groups, but no significant variations between CK and top/mid groups. Pielou's evenness index suggested reduced community uniformity in the bottom group due to partial dominance of specific bacterial taxa, whereas no dominant taxa were evident in other groups.

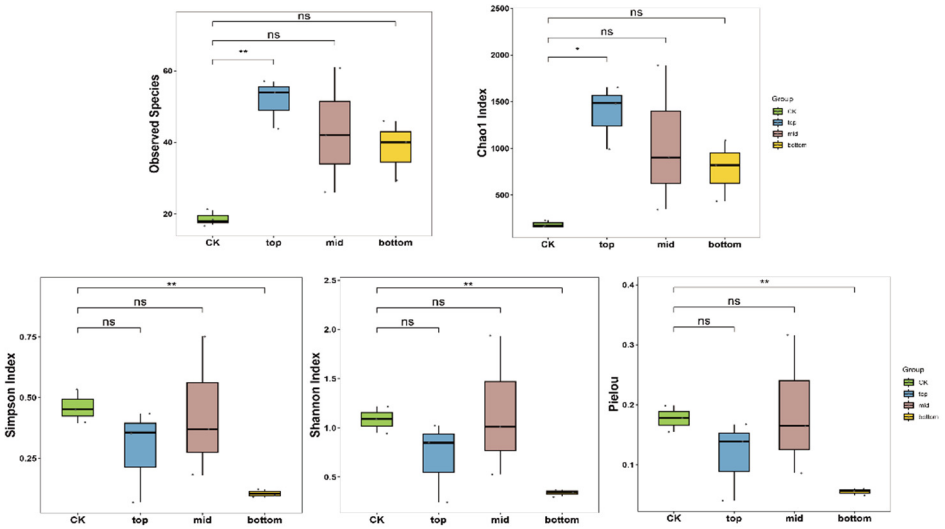

Figure 6. Bacterial alpha diversity index analysis (* represents the significance of diversity index difference between different treatments. *, $p < 0.05$; **, $p < 0.01$)

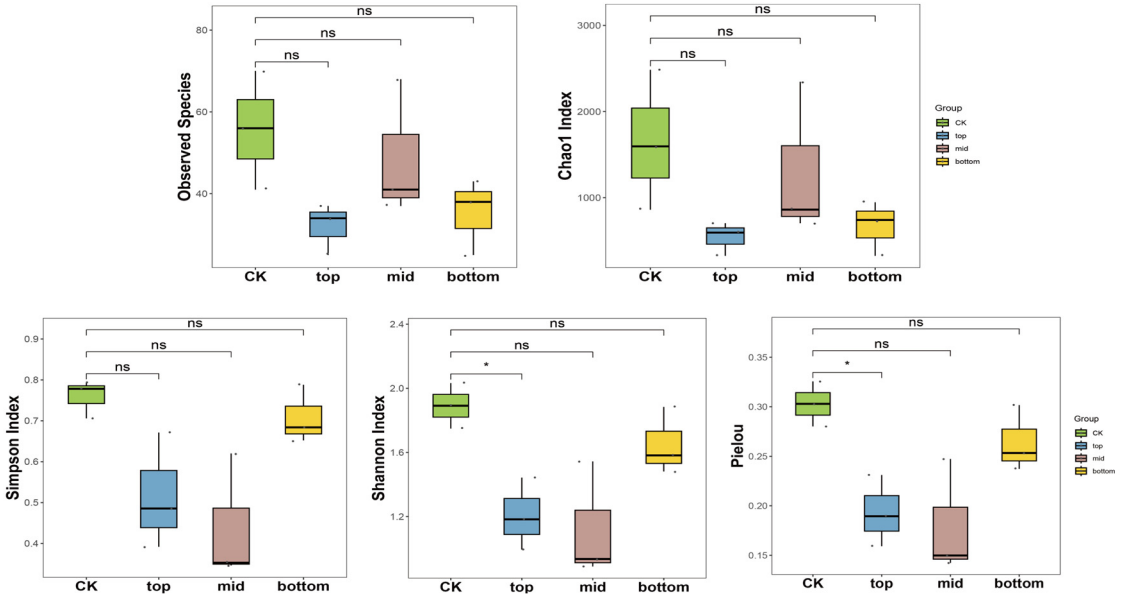

Figure 7. Fungal alpha diversity index analysis (* represents the significance of diversity index difference between different treatments. *, $p < 0.05$; **, $p < 0.01$, ***, $p < 0.001$).)

For fungal communities (Figure 7), decayed groups displayed lower Observed and Chao1 indices than the CK group, reflecting decreased fungal species richness during spoilage, though no significant intergroup differences were detected. Diversity indices (Simpson and Shannon) revealed higher fungal diversity in CK and bottom groups compared to other groups. A significant difference in Shannon index emerged between CK and top groups, but not among CK, mid, and bottom groups. Pielou's index implied reduced evenness in top and mid groups due to dominance of specific fungal

taxa, whereas CK and bottom groups likely maintained balanced fungal communities without pronounced dominance.

3.4. Beta Diversity of Microbial Communities in Decayed Wax Apples

For bacterial communities (Figure 8), Bray-Curtis dissimilarity analysis revealed significant intergroup differences (Adonis test: $R^2 = 0.5061$, $p < 0.001$), with PCoA1 and PCoA2 axes explaining 55.74% and 25.79% of total variance, respectively. Similarly, Jaccard distance-based analysis confirmed pronounced divergence (Adonis test: $R^2 = 0.6474$, $p < 0.001$), where PCoA1 and PCoA2 accounted for 46.25% and 24.24% of variance. Both metrics demonstrated statistically robust separation among groups ($p < 0.001$).

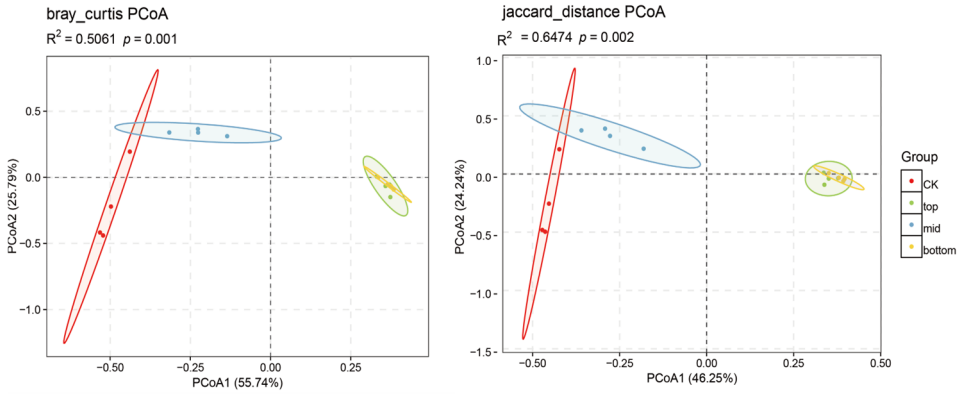

Figure 8. Bacterial principal coordinate analysis (PCoA) based on Bray-Curtis and Jaccard distance

For fungal communities (Figure 9), Bray-Curtis analysis showed stronger intergroup discrimination (Adonis test: $R^2 = 0.7481$, $p < 0.001$), with PCoA1 (43.03%) and PCoA2 (34.65%) capturing the majority of variance. Jaccard distance analysis yielded comparable results (Adonis test: $R^2 = 0.6455$, $p < 0.001$), where PCoA1 (36.11%) and PCoA2 (26.5%) explained 62.61% cumulative variance. Both approaches validated extreme significance in fungal community differentiation across groups ($p < 0.001$).

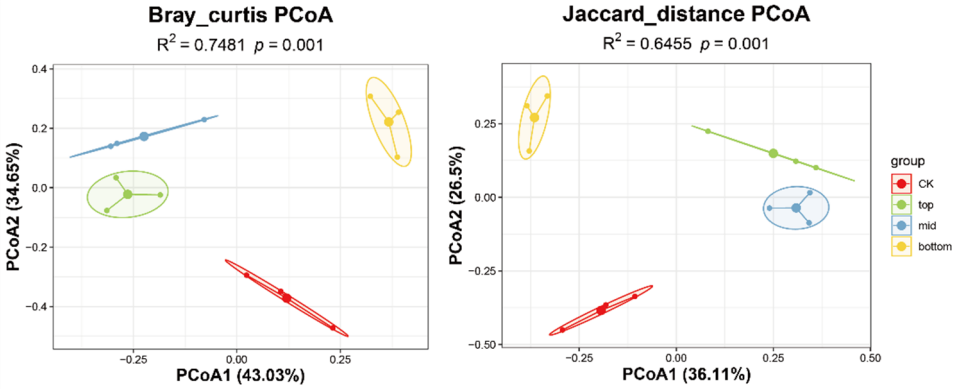

Figure 9. Fungal principal coordinate analysis (PCoA) based on Bray-Curtis and Jaccard distance

3.5. Microbial Community LEfSe Analysis of Decayed Wax Apple Samples

As illustrated in Figures 10 and 11, significant indicator species in fungal communities across different decayed regions exhibited notable differences. Two differentially abundant fungal taxa with LDA >5 ($p<0.05$) was identified at species level: Colletotrichum coccodes in the top region and Colletotrichum tropicicola in the bottom region. These species exhibited the highest relative abundances in their respective groups and are postulated to play predominant roles in group-specific biological processes.

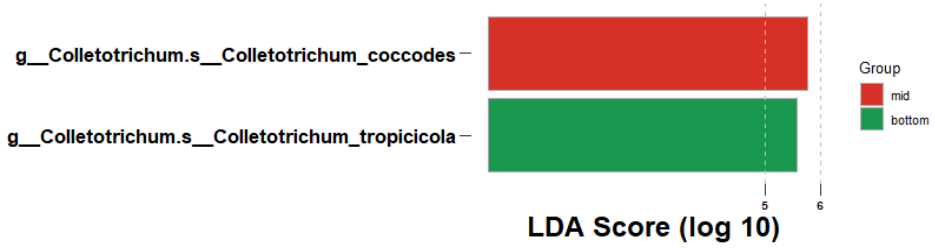

Figure 10. LEfSe analysis of the fungal community across different health conditions and three distinct stages of decay in wax apple samples: The distribution of LDA scores for differential species, with colors representing the corresponding groups, and the length of the bars indicating the contribution of differential species (namely, LDA score).

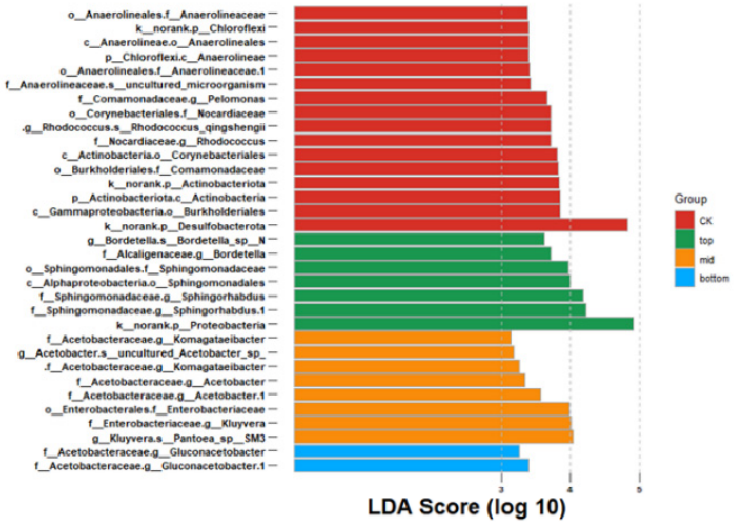

Figure 11. LEfSe analysis of the bacterial community across different health conditions and three distinct stages of decay in *Syzygium samarangense* samples: Multilevel linear discriminant analysis (LDA) of differential species. The distribution of LDA scores for differential species, with colors representing the corresponding groups, and the length of the bars indicating the contribution of differential species (namely, LDA score)

In bacterial communities, significant inter-regional variations were observed (LDA >3, $p<0.05$). The top region demonstrated significant enrichment of Proteobacteria phylum, Sphingorhabdus and Bordetella genera. The mid-region showed predominant abundance of Kluyvera and Acetobacter genera, while the bottom region was characterized by Gluconobacter genus. Notably, the healthy wax apple group exhibited marked enrichment of Desulfobacterota phylum compared to decayed samples.

3.6. Functional Prediction of Microbial Communities in Decayed Wax Apple Samples Using PICRUSt2

3.6.1. KEGG-based Metabolic Pathway Analysis

The predicted bacterial functional profiles at KEGG level 2 are shown in Figure 12. In healthy wax apples, bacterial functions were significantly enriched in terpenoid and polyketide metabolism, energy metabolism, and excretory systems. The terpenoid and polyketide metabolism likely synthesizes antimicrobial or antioxidative compounds to inhibit pathogenic microbial growth, while the excretory system may facilitate the removal of metabolic waste, maintaining intracellular homeostasis and preventing toxic substance accumulation. These mechanisms suggest that the healthy tissues sustain microbial ecological balance through basal metabolism and antimicrobial compound synthesis.

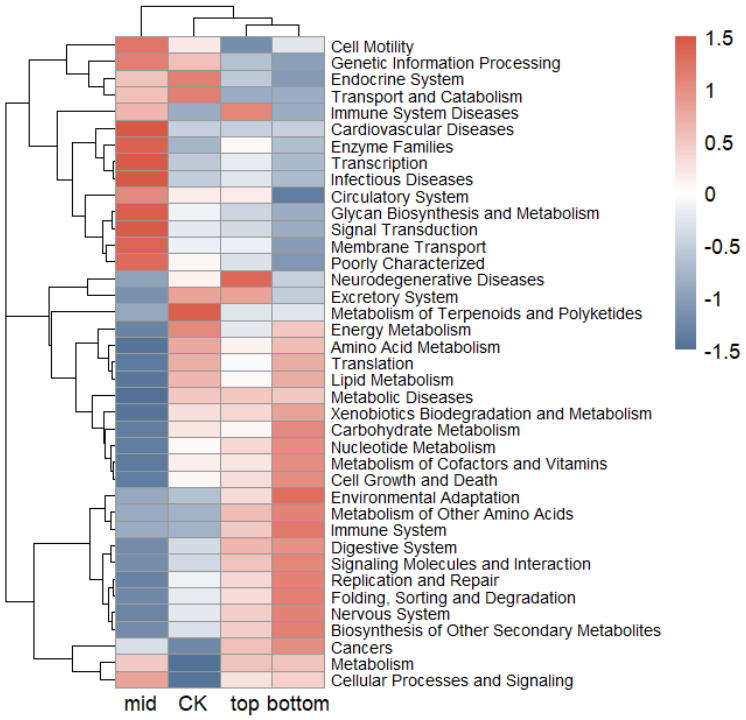

Figure 12. Analysis of secondary metabolic pathways based on the KEGG database

In contrast, decayed regions exhibited functional enrichment in membrane transport, cellular motility, signal

transduction, xenobiotic degradation, and immune systems. Notably, the enhanced activity of the type III secretion system (a membrane transport pathway) may translocate effector proteins into host cells to disrupt immunity. Signal transduction pathways, including quorum sensing regulation, could coordinate virulence gene expression. Xenobiotic degradation pathways may degrade host-derived defensive secondary metabolites to weaken disease resistance. Elevated immune system-related functions might promote bacterial survival by interfering with host immune signaling. These findings collectively indicate that bacterial communities accelerate wax apple decay by enhancing virulence expression and disrupting host immune responses.

3.6.2. METACYC Database Annotation Analysis

As shown in Figure 12, the metabolic pathways of fungal communities in wax apple samples were annotated using the METACYC database. In healthy tissues, the top three enriched fungal pathways were superpathways, pyrimidine metabolism, and aerobic respiration I (cytochrome pathway), indicating that fungi in healthy regions primarily engage in basal metabolism, utilizing host-derived carbon sources without activating pathogenesis-related pathways.

In contrast, fungal communities in decayed tissues exhibited significant upregulation of the glyoxylate cycle, galactose degradation, mevalonate pathway, pantothenate and heme biosynthesis, 4-aminobutyrate degradation, and GDP-mannose biosynthesis pathways compared to healthy samples. These changes reveal pathogenic strategies: At the first, the glyoxylate cycle and galactose degradation suggest fungal utilization of host fatty acids and galactose as carbon sources for energy production. In the second, the mevalonate pathway facilitates isoprenoid synthesis, while pantothenate (a precursor of coenzyme A) and heme biosynthesis may enhance toxin production to promote host invasion. Heme could further degrade defensive phenolic compounds or synthesize mycotoxins to accelerate decay. Then, degradation of 4-aminobutyrate may suppress host immune responses. At last, GDP-mannose biosynthesis likely strengthens fungal cell walls via mannan synthesis, resisting host enzymatic degradation. These results collectively demonstrate that fungi adapt to the wax apple microenvironment and drive decay by activating pathways linked to carbon source exploitation, toxin synthesis, antioxidant defense, and immune evasion.

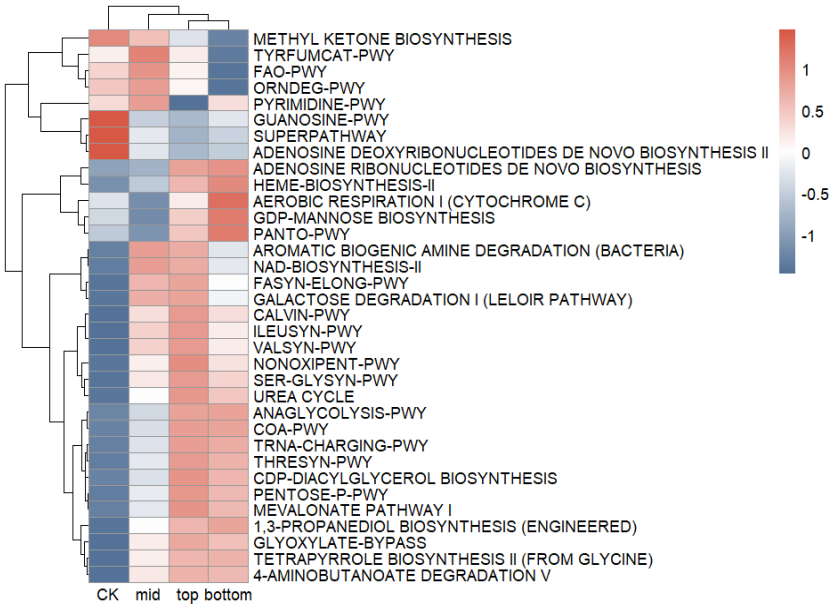

Figure 13. Metabolic pathway analysis based on the METACYC database

4. Discussion

High-throughput sequencing and community analysis revealed that bacterial diversity increased during wax apple decay, while fungal diversity decreased. Post-decay, both bacterial and fungal communities exhibited reduced diversity, indicating potential dominance of specific microbial taxa—a trend consistent with microbial dynamics observed during grape and blueberry decay [8, 14].

Although microbial community structures differed significantly between healthy and decayed regions (top, mid, bottom), analysis of highly abundant taxa suggested relatively low bacterial pathogenicity. In contrast, fungal invasion—commonly reported in wax apples, papayas, plums, grapes, and other fruits—is often linked to cellular damage and subsequent microbial colonization [15-18]. This supports the hypothesis that fungal activity initiates wax apple decay, with secondary microbial invasion following host tissue compromise.

Healthy wax apple tissues exhibited enrichment in excretory systems and energy metabolism pathways, reflecting their reliance on basal metabolism and antimicrobial compound synthesis to maintain microecological balance. In decayed regions, bacterial communities showed upregulated functions in membrane transport, cellular motility, signal transduction, xenobiotic degradation, and immune systems. Similar metabolic shifts have been documented in studies of spoilage-associated bacteria in edible mushrooms [19], suggesting conserved mechanisms where bacterial virulence and host immune interference accelerate decay.

Concurrently, decay-associated fungi displayed marked activation of glyoxylate cycle, galactose degradation, mevalonate pathway, pantothenate/heme biosynthesis, 4-aminobutyrate degradation, and GDP-mannose biosynthesis. These pathways align with strategies for carbon scavenging, toxin synthesis, antioxidant defense, and immune evasion, mirroring Botrytis cinerea pathogenesis in grape berries

during gray mold development [20]. Furthermore, bacterial pectinases and cellulases likely degrade fruit cell walls, releasing monosaccharides and fatty acids to fuel fungal growth [21], while fungal metabolites from polysaccharide degradation may reciprocally support bacterial proliferation. This cross-kingdom synergy drives the progression of wax apple decay.

References

[1] Banadka A, Wudali N.S, Alkhayri J.M, et al. The role of Syzygium samarangense in nutrition and economy: An overview [J]. South African Journal of Botany, 2022, 145(8): 481-492.

[2] Zakaria L. Diversity of Colletotrichum Species Associated with Anthracnose Disease in Tropical Fruit Crops-A Review [J]. Agriculture, 2021, 11(4):297-299.

[3] Lin Y, Yang L, Qiu S, et al. Rapid Identification and Source Tracing of a Salmonella Typhimurium Outbreak in China by Metagenomic and Whole-Genome Sequencing [J]. Foodborne Pathogens and Disease, 2022, 19(4): 259-265.

[4] Billington C, Kingsbury J.M, Rivas L. Metagenomics Approaches for Improving Food Safety: A Review [J]. Journal of Food Protection, 2022, 85(3): 448-464.

[5] Zhao L, Li H, Liu Z, et al. Quality Changes and Fungal Microbiota Dynamics in Stored Jujube Fruits: Insights from High-Throughput Sequencing for Food Preservation [J]. Foods , 2024, 13(10): 1473-1475.

[6] Zhao Q, Shi Y, Ngea G.L, et al. Changes of the microbial community in kiwifruit during storage after postharvest application of Wickerhamomyces anomalus [J]. Food Chemistry, 2023, 404(3): 134593.

[7] Xu H, Quan Q, Xie Y, et al. Unraveling and comparing bacterial community signatures and functions of postharvest strawberries packaged with different films during storage [J]. Lebensmittel Wissenschaft und Technologie Food Science and Technology, 2024, 199(5): 116078.

[8] Wang J, Shi C, Fang D, et al. The Impact of Storage Temperature on the Development of Microbial Communities on the Surface of Blueberry Fruit [J]. Foods , 2023, 12(8):1611-1613.

[9] Liu Y, Zhang L, Hu T, et al. A New Strategy for Enhancing Postharvest Quality of Sweet Cherry: High-Voltage Electrostatic Field Improves the Physicochemical Properties and Fungal Community [J]. Foods, 2024, 13(22): 3670-3672.

[10] Callahan B.J, Mcmurdie P.J, Rosen M.J, et al. DADA2: High-resolution sample inference from Illumina amplicon data [J]. Nature Methods, 2016, 13(7): 581-588.

[11] Xueyao Gao, Xianming Yang, Yanhui Lu, et al. Infection of the symbiotic bacterium Asaia in four Lepidoptera pests [J]. Journal of Applied Entomology, 2016, 53(04): 830-836.

[12] Van W.N, Badura J, Von W.C, et al. Exploring future applications of the apiculate yeast Hanseniaspora [J]. Critical Reviews in Biotechnology, 2024, 44(1): 100-119.

[13] Wanhai Li. Biological control of postharvest green mold on citrus with Saccharomyces cerevisiae combined with lecithin from grape juice and its mechanism [D], Jiangsu University, 2016.

[14] Hailian Zhou. Study on the inhibitory mechanism of Hanseniaspora uvarum on gray mold disease [D], Nanjing Agricultural University, 2012.

[15] Yao Y, Zhao M, He P.B, et al. First report of Colletotrichum siamense as a causal agent of anthracnose on wax apple (Syzygium samarangense) in China [J]. Plant disease, 2023, 107(12): 0191-0217.

[16] Wang R, Ouyang D, Lu M, et al. Identification and Characterization of Colletotrichum Species Associated with Anthracnose Disease of Plum [J]. Plant Disease, 2024, 108(9): 2874-2886.

[17] Vieira D.S, Veloso J.S, Dasilva A.C, et al. Elucidating the Colletotrichum spp. diversity responsible for papaya anthracnose in Brazil [J]. Fungal Biology, 2022, 126(10): 623-630.

[18] Steiner D.R, Modesto L.R, Dias A.H, et al. Colletotrichum nymphaeae and Colletotrichum theobromicola isolated from anthracnose symptoms cause grape ripe rot [J]. Plant Pathology, 2024, 74(3): 813-824.

[19] Xia F, Zhang C.C, Jiang Q.Y, et al. Microbiome analysis and growth behaviors prediction of potential spoilage bacteria inhabiting harvested edible mushrooms [J]. Journal of Plant Diseases and Protection, 2024, 131(1): 77-90.

[20] Váczy K.Z, Otto M, Gomba-Tóth A, et al. Botrytis cinerea causes different plant responses in grape (Vitis vinifera) berries during noble and grey rot: diverse metabolism versus simple defence [J]. Frontiers in Plant Science, 2024, 15(10): 1433161.

[21] Wei C.H, Liu M.Q, Meng G.L, et al. Characterization of Endofungal Bacteria and Their Role in the Ectomycorrhizal Fungus Helvella bachu [J]. Journal of Fungi, 2024, 10(12): 889-893.